

BRIEF NOTE

Evaluation of contrast enhancement ultrasound images of Sonazoid microbubbles in tissue-mimicking phantom obtained by optimal Golay pulse compression

To cite this article: Shinnosuke Hirata *et al* 2022 *Jpn. J. Appl. Phys.* **61** SG1015

View the [article online](#) for updates and enhancements.

You may also like

- [Complex behaviour in optical systems and applications](#)
Wulfhard Lange and Thorsten Ackemann
- [Nonlinear transverse vibration of nano-strings based on the differential type of nonlocal theory](#)
P Y Wang, C X Zhu, C Li et al.
- [Strong nonlinear focusing of light in nonlinearly controlled electromagnetic active metamaterial field concentrators](#)
Yu G Rapoport, A D Boardman, V V Grimalsky et al.



Evaluation of contrast enhancement ultrasound images of Sonazoid microbubbles in tissue-mimicking phantom obtained by optimal Golay pulse compression

Shinnosuke Hirata^{1*}, Yuki Hagihara², Kenji Yoshida¹, Tadashi Yamaguchi¹, Matthieu E. G. Toulemonde³, and Meng-Xing Tang³

¹Center for Frontier Medical Engineering, Chiba University, Chiba 263-8522, Japan

²Department of Medical Engineering, Chiba University, Chiba 263-8522, Japan

³Department of Bioengineering, Imperial College London, London, SW7 2AZ, United Kingdom

*E-mail: shin@chiba-u.jp

Received November 3, 2021; revised December 24, 2021; accepted January 10, 2022; published online March 22, 2022

In contrast enhancement ultrasound (CEUS), the vasculature image can be formed from nonlinear echoes arising from microbubbles in a blood flow. The use of binary-coded pulse compression is promising for improving the contrast of CEUS images by suppressing background noise. However, the amplitudes of nonlinear echoes can be reduced, and sidelobes by nonlinear echoes can occur depending on the binary code. Optimal Golay codes with slight nonlinear-echo reduction and nonlinear sidelobe have been proposed. In this study, CEUS images obtained by optimal Golay pulse compression are evaluated through experiments using Sonazoid microbubbles flowing in a tissue-mimicking phantom.
© 2022 The Japan Society of Applied Physics

In contrast enhancement ultrasound (CEUS), nonlinear echoes from microbubbles (MBs) in a blood flow are used for contrast-specific image construction. CEUS images are useful for visualizing the blood flow and are promising for vasculature evaluation.¹⁻⁹⁾ These MBs, called ultrasound contrast agents (UCAs), comprise gas cores encapsulated in shells.¹⁰⁾ The contrast of the CEUS image is further enhanced when the amplitude of ultrasound increases. However, MBs can be destroyed by the use of even moderate-amplitude ultrasound.¹¹⁾ To relatively improve the contrast of CEUS images without increasing the amplitude of ultrasound, pulse compression using a frequency-modulated (FM) signal or binary-coded (BC) sequence has been introduced.^{12,13)} In pulse compression, the received FM echo or BC echo sequence is compressed to a short pulse by the cross-correlation between the received signal and the reference signal that corresponds to the transmitted signal. Furthermore, the background noise in the received signal is suppressed by cross-correlation. Therefore, the signal-to-noise ratio of the echo is improved, i.e. the image contrast is relatively improved. However, these pulse compression algorithms function effectively for linear echoes. In terms of nonlinear echoes from MBs, a sidelobe can occur around the compressed short pulse (correlation peak), and the peak amplitude that corresponds to the MB contrast can also be reduced, particularly in BC pulse compression. Previously, an estimation method of the nonlinear-peak reduction and the nonlinear sidelobe shape has been proposed.¹⁴⁾ Furthermore, optimal Golay codes for CEUS with slight nonlinear-peak reduction and nonlinear sidelobe have been identified from all patterns of Golay codes.¹⁵⁾ However, the proposed Golay pulse compression for CEUS has been verified in only RF echo data obtained via computer simulations based on single MB oscillations or experiments using a silicone tube filled with MB suspension in water.^{14,16)} Therefore, in this study, CEUS images obtained by optimal Golay pulse compression were evaluated through experiments using a silicone tube filled with MB suspension in a tissue-mimicking phantom.

The experimental configuration used in this study is illustrated in Fig. 1. A tissue-mimicking phantom with flow channels was formed in the resin mold. The agar portion was composed of 92.5 wt% ultrapure water, 5 wt% of nylon

particles with a diameter of 5 μm (ORGASOL 2002 EXD NAT 1, Arkema, France) as scatterers, 2 wt% agar powder (Agar, Sigma-Aldrich, USA), and 0.5 wt% surfactant (TERGITOL Type NP-10, Sigma-Aldrich, USA). Silicone tubes with an inner diameter of 0.3 mm and outer diameter of 0.4 mm (Aramec silicone micro tube, Aram, Japan) were placed at distances 30 and 50 mm from the top surface of the phantom. Sonazoid, which is the UCA used for the diagnosis of focal liver lesions in Japan, was used in the experiment.^{17,18)} The Sonazoid suspension for injection was diluted 100 times and manually flushed into the tube using a syringe. The transmission of the BC ultrasound and acquisition of echoes were performed using a research ultrasound system (Vantage 256, Verasonics, USA). A linear array probe (L11-5v, Verasonics, USA) was mounted on the system. The probe was placed above each silicone tube in the longitudinal direction. To form CEUS images, pulse-inverted amplitude modulation (PIAM) was employed.^{19,20)} Moreover, three-times transmissions by the negative pulse from odd number elements, the positive pulse from all elements, and the negative pulse from even number elements were employed to ease transmission of half-amplitude ultrasound in the PIAM. The positive and negative pulses with a center frequency of 5 MHz were transmitted as plane waves via PWM excitations. In terms of Golay pulse compression, the sequences composed of positive and negative pulses were transmitted as Golay codes A and B, and the pulse interval was set to 2 μs . In the experiments, CEUS images formed by the proposed method, which is the PIAM with Golay pulse compression, were compared with those obtained using the conventional PIAM. Therefore, nine sequences of transmission/acquisition were repeated. The first three sequences corresponded to the conventional PIAM. The next three sequences corresponded to PIAM with Golay code A (fifth sequence) and inverted Golay code A' (fourth and sixth sequences). The last three sequences corresponded to PIAM with Golay code B (eighth sequence) and inverted Golay code B' (seventh and ninth sequences). In this study, Golay codes A' and B', which were mirrored Golay codes A and B, were used to create a small nonlinear sidelobe.¹⁴⁾ The repetition frequency of these consecutive sequences was

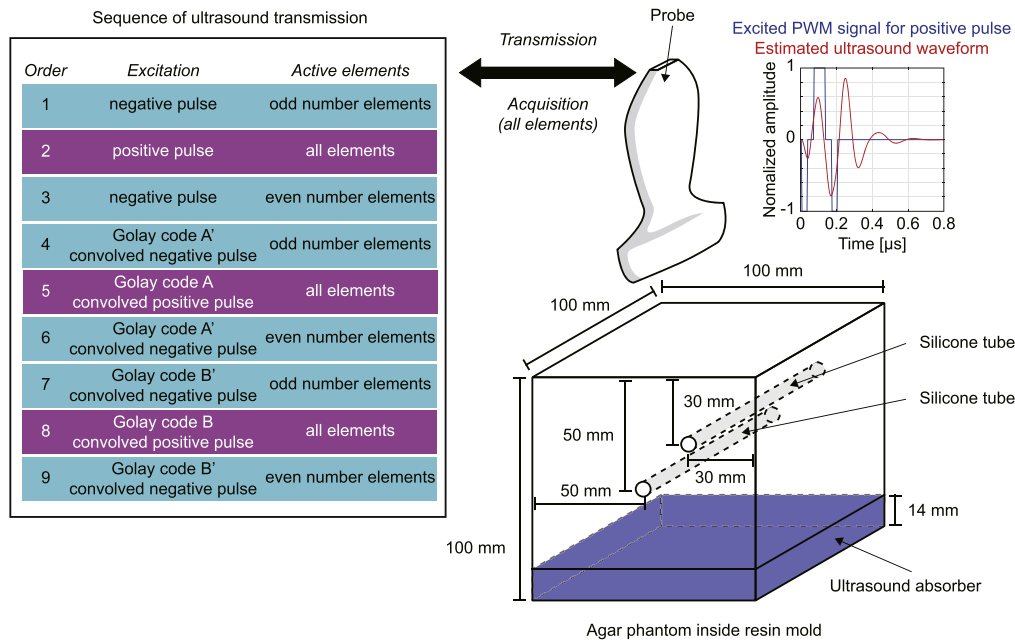


Fig. 1. (Color online) Experimental setup and sequence of ultrasound transmission/acquisition.

100 Hz. Therefore, the frame rate of the CEUS images was 11.1 fps. The other parameters are listed in Table I.

When the Sonazoid suspension was flowing at a depth of 30 mm, the conventional B-mode image that represents the amplitudes of the RF echo data acquired by the second sequence is shown in Fig. 2(a). The conventional PIAM image formed from the summation of the RF echo data acquired by the first, second, and third sequences is shown in Fig. 2(b). In both images, high contrast lines were observed at approximate depth of 32 mm. The mean brightness within ± 10 mm lateral in these images is shown in Figs. 2(d) and 2(e). The linear echoes from the scatterers were reduced by approximately 16 dB by the PIAM of this system. However, the nonlinear echoes from the Sonazoid MBs were not reduced, whereas the two peaks at depths of 32.1 and 32.6 mm were reduced to the same level. Therefore, the two peaks appeared to be linear echoes from the outer surface of the upper wall and the inner surface of the lower wall of the silicone tube. The nonlinear echoes from the Sonazoid MBs appeared between the two peaks. To further reduce the linear echoes from the silicone tube, the moving target indicator (MTI), which is the subtraction of two RF echo data from adjacent frames, was applied. The static components that corresponded to the linear echoes in the experiments can be reduced by the MTI. The conventional PIAM image with the MTI is shown in Fig. 2(c), and the mean brightness in the image is indicated in Figs. 2(d) and 2(e). The nonlinear echoes from the Sonazoid MBs can be obtained at a depth of 32.4 mm, and its contrast from the background noise level was approximately 13 dB. Meanwhile, the B-mode image with Golay pulse compression formed from the summation of cross-correlation functions of the fifth and eighth sequences is shown in Fig. 2(f). The PIAM image with Golay pulse compression formed from the summation of cross-correlation functions from fourth to ninth sequences is shown in Fig. 2(g). In the case of the PIAM image with Golay pulse compression, the background noise level decreased by approximately 13 dB, which is

Table I. Parameters of ultrasound transmission/acquisition.

Elements of transducer	128
Element pitch	0.3 mm
Voltage of PWM excitation	8.2 V
Estimated sound pressure	0.225 MPa at depth of 50 mm
Sampling frequency	50 MHz
Center frequency of pulse	5 MHz
Pulse (sequence) repetition frequency	100 Hz
Golay code A	-1 -1 1 1 1 1 1 -1 1 1
Golay code B	1 1 -1 1 -1 1 -1 -1 1 1
Golay code A' (mirrored A)	1 1 -1 1 1 1 1 -1 -1
Golay code B' (mirrored B)	1 1 -1 -1 1 -1 1 -1 1 1
Interval of binary pulses	2 μ s

equivalent to the theoretical value of 10-bit Golay codes, in the deep region. The PIAM image with Golay pulse compression and the MTI is shown in Fig. 2(h). In the B-mode and PIAM images, the peak amplitudes of the conventional and proposed methods were similar. In the PIAM images with the MTI, however, the peak amplitude of the proposed method was smaller than that of the conventional method. Hence, the nonlinear echoes from the Sonazoid MBs decreased approximately 3 dB by the nonlinear peak reduction of pulse compression using 10-bit optimal Golay codes. Furthermore, the nonlinear sidelobe appeared from 21 to 46 mm in depth. The nonlinear echoes that corresponded to the actual flow of the Sonazoid MBs were approximately 10 dB greater than the maximum nonlinear sidelobe that generates artifacts of the flow. Therefore, the contrast from the background noise level was improved by Golay pulse compression, but the appearance of artifacts may be an issue.

The conventional B-mode and PIAM images and the PIAM image with the MTI when the Sonazoid suspension was flowing at a depth of 50 mm are shown in Figs. 3(a)–3(c). The mean brightness in the images is shown in

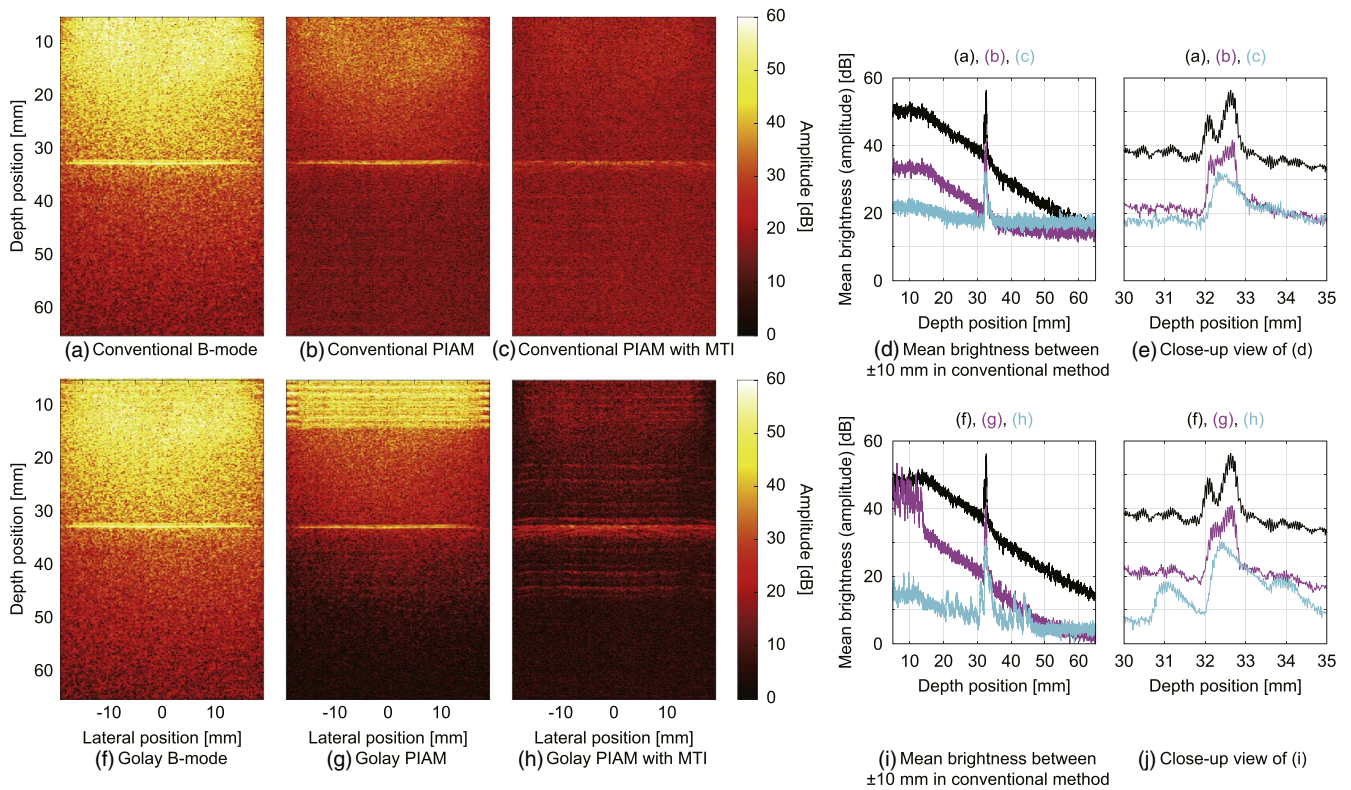


Fig. 2. (Color online) Experimental results based on Sonazoid suspension flowing at depth of 30 mm in tissue-mimicking phantom.

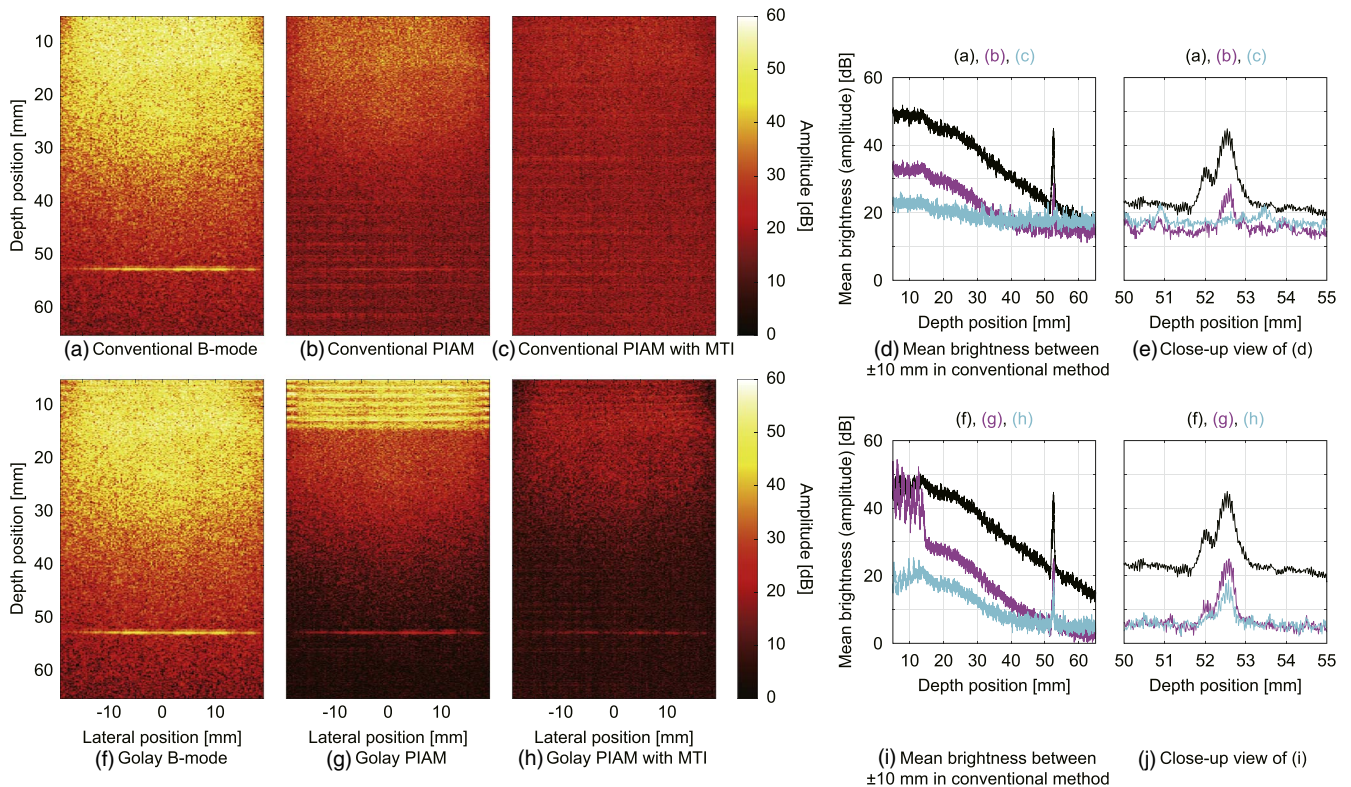


Fig. 3. (Color online) Experimental results based on Sonazoid suspension flowing at depth of 50 mm in tissue-mimicking phantom.

Figs. 3(d) and 3(e). The linear echoes from the scatterers and the tube wall were reduced by the PIAM and MTI. However, the nonlinear echoes from the Sonazoid MBs could not be determined by the background noise. The B-mode and PIAM images and the PIAM image with the MTI with Golay pulse compression are shown in Figs. 3(f)–3(h), and the

corresponding mean brightness is shown in Figs. 3(i) and 3(j), respectively. The nonlinear echoes from the Sonazoid MBs can be obtained at a depth of 52.5 mm, and its contrast from the background noise level was approximately 12 dB. Therefore, nonlinear echoes could not be obtained in the conventional PIAM with the MTI image, and nonlinear

sidelobes that appeared similar to the background noise could not be identified.

In this study, CEUS images of the Sonazoid MB in the tissue-mimicking phantom were formed by pulse compression using 10-bit optimal Golay codes, PIAM of three-times transmissions, and the MTI. In the CEUS image, the background noise level decreased by approximately 13 dB. Subsequently, the nonlinear echoes from the Sonazoid MBs decreased by approximately 3 dB. Therefore, the contrast of the CEUS image improved by approximately 10 dB. However, the nonlinear sidelobe, which was 10 dB smaller than the nonlinear echoes, appeared around the actual flow.

Acknowledgments This study was partly supported by the Japan Society for the Promotion of Science Core-to-Core Program JPJSCCA20170004.

ORCID iDs Shinnosuke Hirata  <https://orcid.org/0000-0001-6940-3287> Matthieu E. G. Toulemonde  <https://orcid.org/0000-0002-3191-8020> Meng-Xing Tang  <https://orcid.org/0000-0001-7686-425X>

- 1) C. Tremblay-Darveau, R. Williams, L. Milot, M. Bruce, and P. N. Burns, *IEEE Trans. Med. Imaging* **35**, 699 (2016).
- 2) A. Stanzola, C. H. Leow, E. Bazigou, P. D. Weinberg, and M. X. Tang, *IEEE Trans. Med. Imaging* **37**, 1847 (2018).
- 3) A. Bar-Zion, C. Tremblay-Darveau, O. Solomon, D. Adam, and Y. C. Eldar, *IEEE Trans. Med. Imaging* **36**, 169 (2017).
- 4) D. H. Simpson, C. T. Chin, and P. N. Burns, *IEEE Trans. Ultrason. Ferroelectr. Freq. Control* **46**, 372 (1999).
- 5) C. H. Leow and M. X. Tang, *Ultrasound Med. Biol.* **44**, 134 (2018).
- 6) M. E. G. Toulemonde et al., *JACC: Cardiovasc. Imaging* **11**, 923 (2018).
- 7) J. Voorneveld et al., *Circ. Cardiovasc. Imaging* **12**, e008856 (2019).
- 8) K. Yoshida, K. Saito, M. Omura, and T. Yamaguchi, *Jpn. J. Appl. Phys.* **59**, SKKE07 (2020).
- 9) H. J. Vos, J. D. Voorneveld, E. Groot Jebbink, C. H. Leow, L. Nie, A. E. van den Bosch, M. X. Tang, S. Freear, and J. G. Bosch, *Ultrasound Med. Biol.* **46**, 2875 (2020).
- 10) D. Cosgrove, *Eur. J. Radiol.* **60**, 324 (2006).
- 11) M. X. Tang, N. Kamiyama, and R. J. Eckersley, *Ultrasound Med. Biol.* **36**, 459 (2010).
- 12) J. M. G. Borsboom, C. T. Chin, A. Bouakaz, M. Versluis, and N. de Jong, *IEEE Trans. Ultrason. Ferroelectr. Freq. Control* **52**, 241 (2005).
- 13) R. J. Eckersley, M. X. Tang, K. Chetty, and J. V. Hajnal, *Ultrasound Med. Biol.* **33**, 1787 (2007).
- 14) S. Hirata, C. H. Leow, M. E. G. Toulemonde, and M. X. Tang, *Jpn. J. Appl. Phys.* **60**, 066501 (2021).
- 15) M. J. E. Golay, *IRE Trans. Inform. Theory* **7**, 82 (1961).
- 16) S. Hirata, Y. Hagihara, K. Yoshida, T. Yamaguchi, M. E. G. Toulemonde, and M. X. Tang, *Proc. Symp. Ultrason. Electron.*, 2E2, 2021.
- 17) P. C. Sontum, *Ultrasound Med. Biol.* **34**, 824 (2008).
- 18) M. Kudo, K. Hatanaka, and K. Maekawa, *J. Med. Ultrasound* **16**, 130 (2008).
- 19) P. J. Phillips, *Proc. IEEE Ultrason. Sympos.*, p. 1739, 2001, 10.1109/ULTSYM.2001.992057.
- 20) R. J. Eckersley, C. T. Chin, and P. N. Burns, *Ultrasound Med. Biol.* **31**, 213 (2005).